

# Predicting Time to Castration Resistance in Hormone Sensitive Prostate Cancer by a Personalization Algorithm Based on a Mechanistic Model Integrating Patient Data

Moran Elishmereni,<sup>1,2</sup> Yuri Kheifetz,<sup>2</sup> Ilan Shukrun,<sup>2</sup> Graham H. Bevan,<sup>3</sup> Debashis Nandy,<sup>3</sup> Kyle M. McKenzie,<sup>3</sup> Manish Kohli,<sup>3\*</sup> and Zvia Agur<sup>1,2\*</sup>

<sup>1</sup>*Institute for Medical Biomathematics (IMBM), Bene Ataroth, Israel*

<sup>2</sup>*Optimata Ltd., Bene Ataroth, Israel*

<sup>3</sup>*Mayo Clinic, Rochester, Minnesota*

**BACKGROUND.** Prostate cancer (PCa) is a leading cause of cancer death of men worldwide. In hormone-sensitive prostate cancer (HSPC), androgen deprivation therapy (ADT) is widely used, but an eventual failure on ADT heralds the passage to the castration-resistant prostate cancer (CRPC) stage. Because predicting time to failure on ADT would allow improved planning of personal treatment strategy, we aimed to develop a predictive personalization algorithm for ADT efficacy in HSPC patients.

**METHODS.** A mathematical mechanistic model for HSPC progression and treatment was developed based on the underlying disease dynamics (represented by prostate-specific antigen; PSA) as affected by ADT. Following fine-tuning by a dataset of ADT-treated HSPC patients, the model was embedded in an algorithm, which predicts the patient's time to biochemical failure (BF) based on clinical metrics obtained before or early in-treatment.

**RESULTS.** The mechanistic model, including a tumor growth law with a dynamic power and an elaborate ADT-resistance mechanism, successfully retrieved individual time-courses of PSA ( $R^2 = 0.783$ ). Using the personal Gleason score (GS) and PSA at diagnosis, as well as PSA dynamics from 6 months after ADT onset, and given the full ADT regimen, the personalization algorithm accurately predicted the individual time to BF of ADT in 90% of patients in the retrospective cohort ( $R^2 = 0.98$ ).

**CONCLUSIONS.** The algorithm we have developed, predicting biochemical failure based on routine clinical tests, could be especially useful for patients destined for short-lived ADT responses and quick progression to CRPC. Prospective studies must validate the utility of the algorithm for clinical decision-making. *Prostate* © 2015 Wiley Periodicals, Inc.

**KEY WORDS:** androgen deprivation therapy (ADT); mathematical model; non-linear mixed-effect modeling (NLMEM); biochemical failure (BF); Bayesian estimation

## INTRODUCTION

Prostate cancer (PCa) is the most frequently diagnosed cancer and the sixth leading cause of cancer death in men worldwide. Over 30% of patients progress from localized stage disease to advanced stages over 10 years [1]. Chronic androgen deprivation therapy (ADT) is often used as first-line treatment to control relapse after progression, and for patients diagnosed with metastatic hormone sensitive prostate cancer (HSPC) [2]. ADT suppresses cancer growth by depleting androgen and causing apoptotic regression

---

Conflict of interest: Nothing to declare.

\*Correspondence to: Zvia Agur, Institute for Medical Biomathematics (IMBM), POB 282, Hate'ena St. 10, Bene Ataroth 60991, Israel. E-mail: agur@imbm.org

\*Correspondence to: Manish Kohli, Mayo Clinic, 200 1st St. SW, Rochester, MN 55905. E-mail: Kohli.Manish@mayo.edu

Received 6 July 2015; Accepted 15 September 2015

DOI 10.1002/pros.23099

Published online in Wiley Online Library  
(wileyonlinelibrary.com).

of cancer cells dependent on androgen. This control of PCa progression can last up to several years, until resistance to ADT emerges, and transition to castrate resistant prostate cancer (CRPC) becomes inevitable [3]. In the United States more than one-third of PCa patients undergo ADT at some point, making ADT a significant public health burden due to its adverse effects [4].

An increase in serum prostate-specific antigen (PSA) levels under ADT often heralds disease progression and treatment failure, yet PSA does not help predict the clinical outcome [5]. In fact, today there are no reliable clinical tools that accurately predict ADT failure, in part, due to the large heterogeneity in PSA dynamics among patients [5]. The quest for such methods has become even more essential with the emergence of many novel targeted therapies for HSPC: awareness of a shorter time to progression on ADT may support clinical decision to start novel therapy sooner, rather than delay it to the CRPC stage [2]. To achieve maximal therapeutic gain in HSPC, planning of ADT should be based on predictive and reliable assays of its efficacy in patients [2].

In this work, we aimed to develop a personalization algorithm predicting clinical outcomes in HSPC patients under therapy, based on a mathematical mechanistic model for PCa progression. Mathematical models have been widely employed to predict cancer progression and response to drugs in populations (e.g., [6,7]). We have recently introduced a new approach to PCa immunotherapy by designing a mathematical modelling-based methodology to personalize an experimental vaccination regimen during the initial part of the treatment [8,9]. Here, we have a different aim, namely, to design a method for predicting the response to the standard of care ADT in the individual PCa patient. This aim requires a different methodology and, importantly, relies on the availability of larger clinical databases. Thus, using a hospital-based cohort of HSPC patients, we applied an iterative approach combining non-linear mixed-effect modeling (NLMEM) and dynamic mechanistic modeling for predicting the individual PSA profiles and clinical outcomes in ADT-treated HSPC patients.

## METHODS

### Clinical Data

Information was derived from an advanced stage PCa registry established at Mayo Clinic, consisting of 520 patients recruited between September 2009 and December 2013. An institutional review board

approved access to the de-identified medical records. Patients underwent clinically indicated ADT for HSPC and other treatments for CRPC at Mayo Clinic, and were followed according to the standard of care by individual practitioners experienced in the treatment of advanced PCa. The dataset included basic patient characteristics, full blood biochemistry (with PSA measurements before, during, and after ADT initiation), Gleason score (GS) and Tumor, Nodes, Metastases (TNM) staging at diagnosis, and details of all administered treatments from the time of diagnosis. Available clinical outcomes in these patients included time to biochemical failure (BF) on ADT (defined as two consecutive rises in PSA, at least 1 week apart, according to the clinical standards for biochemical progression [10]), time of CRPC progression (herein defined as the definitive start of chemotherapy after failure of ADT), and survival status.

Patients from the full dataset were stratified by disease stage: those with HSPC treated by ADT, including patients with disease recurrence after primary therapy for localized PCa, were selected as a subset for the present analysis. Criteria for exclusion from this group included fewer than 10 PSA measurements during the HSPC period, or overall PSA dynamics not exceeding 1 ng/ml. This screening resulted in a final subset of  $n=83$  patients (basic descriptors for this cohort are listed in Table I). The applied ADT treatments during the HSPC stage included luteinizing-hormone-releasing hormone agonists and antagonists, with or without anti-androgens, or surgical bilateral orchiectomy (Supplementary Table SI). Longitudinal PSA profiles were assessed from time of HSPC onset (defined as the time of biochemical recurrence or radiological progressive disease after primary therapy for localized PCa, whichever came first), and until time of progression to CRPC or until the last follow-up date (in patients who had not yet progressed to CRPC); the HSPC window is demonstrated in an example PSA profile of a representative patient (Fig. 1). The median time of HSPC follow-up was 3.6 years (Table I). R programming and Excel were used for data analysis.

### Mathematical Mechanistic HSPC Model

The mathematical model of HSPC progression and treatment was developed by an iterative cycle of modeling (designing several different variations of ODE formulations for the ability to retrieve longitudinal PSA profiles in HSPC patients), simulation, fitting to data (comparison of simulated to clinically-observed PSA profiles), and modification

**TABLE I. Descriptors for the HSPC Patient Cohort**

Hormone-sensitive PCa patients (n = 83)	N	%
Age (years), median (range)	66 (43–88)	
BMI, median (range)	29.8 (21.5–41.9)	
Stage at diagnosis, localized PCa/advanced hormone-sensitive PCa	50/33	60/40
PSA <sup>a</sup> at diagnosis (ng/ml), median (range)	18 (2–3,163)	
Gleason score <sup>b</sup> at diagnosis, median (range)	7 (4–9)	
Patients with Gleason score <sup>b</sup> 8–10/≤7	38/41	46/49
Stage M at diagnosis: M0, M1, Mx	23/15/45	28/18/54
Patients on primary therapy for localized PCa (RP/RT)	40/19	48/23
PSA at HSPC onset (ng/ml), median (range)	0.6 (0.1–950)	
HSPC follow up time (years), median (range)	3.6 (0.5–17.7)	
Patients with biochemical failure <sup>c</sup> (BF) on ADT	21	25
Time to BF on ADT (years), median (range)	3.4 (1.1–8.2)	
Patients that progressed to castration-resistant PCa (CRPC) <sup>d</sup>	49	59
Time to CRPC (years), median (range)	3.4 (0.5–17.7)	
Patients alive/deceased	60/23	72/28
Time to death (years), median (range)	5.8 (1.3–18.4)	

PCa, prostate cancer; ADT, androgen deprivation therapy; PSA, prostate-specific antigen.

<sup>a</sup>PSA value unlisted for n = 20 pts.

<sup>b</sup>Gleason score value unlisted for n = 4 pts.

<sup>c</sup>Biochemical failure on ADT defined as two consecutive rises of PSA during ADT.

<sup>d</sup>CRPC diagnosis/onset time defined as start of chemotherapy administration.

for improved retrieval of the data. The final goal was to obtain the simplest model that could retrieve the PSA dynamics in HSPC patients over a substantial time period. The resulting data-adjusted

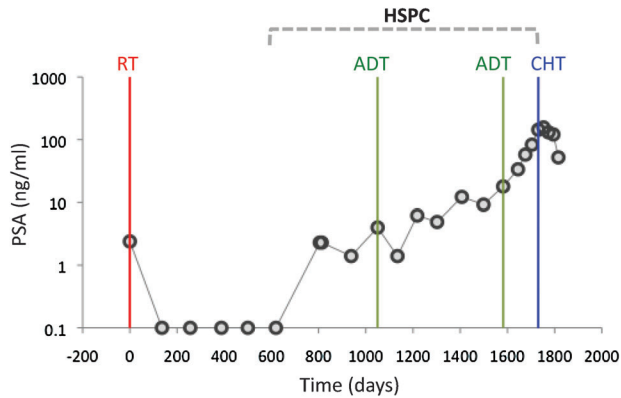


**Fig. 1.** HSPC period of a typical PCa patient's PSA profile. An example PSA profile of a representative patient in the clinical registry dataset is displayed, from the time of diagnosis and until advancement into CRPC. The HSPC onset is defined as the time of biochemical recurrence or radiological progressive disease after primary therapy (e.g. radiation therapy; RT) for localized PCa, whichever came first; The HSPC period ceases upon progression to CRPC (signaled here by chemotherapy; CHT), or until the last follow up date (in patients who had not yet progressed to CRPC). The HSPC period consists of at least one administration of androgen deprivation therapy (ADT).

mechanistic model includes two main components: disease model, describing the dynamics of serum PSA levels taken as proportional to the tumor volume [5]; pharmacodynamics (PD) model of ADT (surgical or medical castration;[11]), which indirectly suppresses androgen levels (represented by testosterone). The model also includes the emergence of ADT resistance during HSPC, whereby PCa progresses even in the presence of sub-castrate levels of androgen; this resistance depends both on androgen receptor (AR)-dependent and independent mechanisms [12,13].

We describe the dynamics of PSA in HSPC by a power growth law with linearly growing power coefficient  $K$ :

$$\frac{dPSA}{dt} = p_0 \cdot \min\left(\frac{\ln(2)}{\gamma}, \lambda_1 \cdot PSA^K\right) \quad (1)$$

$$\frac{dK}{dt} = \lambda_2$$

Here, the parameters  $\lambda_1$  and  $\lambda_2$  stand for the instantaneous rates of increase of  $PSA$  and  $K$ , respectively; parameter  $\gamma$  sets a biologically realistic upper limit on  $PSA$  growth. The model also includes PCa dormancy, i.e., periods of significantly reduced  $PSA$  growth, as often observed in patients. Thus, when  $PSA$  is lower than a given threshold  $p_t$ , parameter  $p_0$  becomes

smaller than unity so that PSA grows considerably more slowly:

$$p_0 = \begin{cases} 1, & \text{PSA} > p_t \\ \left( p + (1-p) \cdot \frac{\text{PSA}}{p_t} \right), & \text{PSA} \leq p_t \end{cases} \quad (2)$$

where parameter  $p$  is the steepness coefficient of the continuous function.

For simplicity, we assumed that the change in testosterone ( $TES$ ) from its homeostatic levels affects PSA linearly, redefining Equation (1) as:

$$\frac{d\text{PSA}}{dt} = p_0 \cdot \min\left(\frac{\ln(2)}{\gamma}, \lambda_1 \cdot \text{PSA}^K\right) + pd_1 \cdot (TES - 1) \cdot \max\left(0, \text{PSA} - \frac{p_t}{2}\right) \quad (3)$$

where the testosterone level is normalized and parameter  $pd_1$  is the rate coefficient for the influence of  $TES$  change on PSA levels. This effect is proportional to PSA levels, and is limited by the half-value of the PSA threshold.

The impact of ADT on testosterone is described by:

$$\frac{dTES}{dt} = \frac{d_{TES}}{1 + pd_3 \cdot H} - d_{TES} \cdot TES \quad (4)$$

$$\frac{dADT}{dt} = -d_1 \cdot ADT \quad (5)$$

$$\frac{dH}{dt} = ADT - d_1 \cdot H \quad (6)$$

In Equation (4), the dynamics of  $TES$  are described by its secretion and removal, parameter  $d_{TES}$  indicating the instantaneous rate of change in the levels of testosterone.  $ADT$  represents any administered hormone deprivation therapy, and its delayed inhibitory effect on  $TES$  production is achieved by an intermediate factor  $H$  (e.g., bound AR). Thus,  $H$  rises as a direct function of  $ADT$  and inhibits  $TES$  production in a saturated manner at the rate  $pd_3$ .  $ADT$  and  $H$  are both cleared at the rate  $d_1$ .

The model allows for the emergence of resistance to ADT:

$$\frac{dRES_1}{dt} = \beta_1 \cdot ADT \quad (7)$$

where  $\beta_1$  is the intrinsic rate of change in the level of resistance per drug unit. To describe the effect of resistance process on  $TES$ , Equation (6) must be redefined:

$$\frac{dH}{dt} = ADT - d_1 \cdot \frac{e^{RES_1}}{1 + e^{RES_1}} \cdot H \quad (8)$$

so that  $RES_1$  increases degradation of  $H$  in a saturated manner, allowing the ADT resistance to interfere with the ADT inhibition of testosterone.

To account for resistance independent of the testosterone-AR pathway, the model includes a second resistance effect,  $RES_2$ :

$$\frac{dRES_2}{dt} = \beta_2 \cdot ADT \quad (9)$$

with  $\beta_2$  as its growth coefficient. This mechanism, describing the direct influence of ADT-associated resistance on PSA, is now incorporated in the PSA function (Equation 3) so that it becomes:

$$\frac{d\text{PSA}}{dt} = p_0 \cdot \min\left(\frac{\ln(2)}{\gamma}, \lambda_1 \cdot \text{PSA}^K\right) + pd_1 \cdot ((TES - 1) + pd_2 \cdot RES_2) \cdot \max\left(0, \text{PSA} - \frac{p_t}{2}\right) \quad (10)$$

Parameter  $pd_2$  is the coefficient through which  $RES_2$  increases PSA growth. The complete system of ODEs is given by:

$$\begin{aligned} \frac{d\text{PSA}}{dt} &= p_0 \cdot \min\left(\frac{\ln(2)}{\gamma}, \lambda_1 \cdot \text{PSA}^K\right) \cdot \frac{\max(0, l_{\text{PSA}} - \text{PSA})}{l_{\text{PSA}}} + \\ &+ pd_1 \cdot \left( (TES - 1) + pd_2 \cdot RES_2 \cdot \frac{\max(0, l_{\text{PSA}} - \text{PSA})}{l_{\text{PSA}}} \right) \cdot \max\left(0, \text{PSA} - \frac{p_t}{2}\right) \\ \frac{dK}{dt} &= \lambda_2, \\ \frac{dTES}{dt} &= \frac{d_{TES}}{1 + pd_3 \cdot H} - d_{TES} \cdot TES \\ \frac{dADT}{dt} &= -d_1 \cdot ADT \\ \frac{dH}{dt} &= ADT - d_1 \cdot \frac{l_h \cdot e^{RES_1}}{l_h + e^{RES_1}} \cdot H \\ \frac{dRES_1}{dt} &= \beta_1 \cdot ADT \cdot \frac{\max(0, l_{\text{res1}} - RES_1)}{l_{\text{res1}}} \\ \frac{dRES_2}{dt} &= \beta_2 \cdot ADT \cdot \frac{\max(0, l_{\text{res2}} - RES_2)}{l_{\text{res2}}} \end{aligned} \quad (11)$$

where  $l_{\text{PSA}}$ ,  $l_h$ ,  $l_{\text{res1}}$ , and  $l_{\text{res2}}$  are biologically reasonable limitation constants on  $PSA$ ,  $H$ ,  $RES_1$ , and  $RES_2$ , respectively.

**Model initial conditions.** Initial conditions for the full model system described in Equation (11) were defined as follows: For flexibility, the initial value of  $PSA$ , which is individualized per patient, was optimized to be close to the baseline  $PSA$  measurement.

Thus:

$$PSA(0) = x_0 \cdot PSA_b \tag{12}$$

where  $PSA_b$  is the individual baseline value of PSA, parameter  $x_0$  is a random variable log normally distributed between 0 and  $\omega_{x_0}$ , with a median value of 1, as given by

$$x_0 \sim e^{N(0, \omega_{x_0})} \tag{13}$$

with  $\omega$  being optimized individually.

The initial value of the power coefficient  $K$ , i.e., parameter  $\alpha$ , was also evaluated from the data, whereas the other variables assume constant initial conditions:

$$K(0) = \alpha, \text{ TES}(0) = 1, \text{ ADT}(0) = 0, \text{ H}(0) = 0, \text{ RES}_2(0) = 0, \text{ RES}_1(0) = 0$$

The model was implemented on a NLMEM platform, and parameters were estimated via the stochastic approximation expectation maximization (SAEM) Monte-Carlo Markov Chain (MCMC) procedure [4,14]. Model agreement with data was evaluated by several criteria, including goodness-of-fit plots, low negative log-likelihood (nLL) values, low Akaike Information Criterion (AIC) values, low relative standard errors (RSE) of parameter estimates, and low condition numbers (CN). Clinical metrics were tested by regression analysis for inclusion as discrete covariates associated with model parameters. See elaborate description of these methods in the Supplementary Material, section A.

### Algorithm-Based Prediction of Biochemical Failure

To predict the time to BF of individual patients after ADT onset, we developed an algorithm that uses personal clinical metrics and the mechanistic HSPC model to forecast patient-specific PSA dynamics. The algorithm, implemented in Matlab employing the MCMC method with the stiff *odes15s* solver, was applied to the cohort's patients. Input data for each patient included GS and initial PSA levels (at diagnosis), PSA measurements at a pre-defined early time period from the ADT onset (i.e. 6 months), and the ADT regimen applied to the patient over the complete follow-up period. Based on the parameter distributions of the population (estimated using data of the full cohort), the algorithm estimated the individual distributions of parameters by MCMC: Fixed parts of individual parameters were estimated according to the regression models on the clinical variables. The random parts of the parameters were sampled accord-

ing to the SAEM algorithm using Bayesian inference [15].

For each patient, 1,000 simulations (each varying in its sampled individual parameter values) were performed. The BF events, as defined above, were extracted from the observed PSA levels, and compared to those in the simulations. A BF event was predicted for a patient only if confirmed in the majority of the simulations (i.e. over half of them; 500 simulations). Comparison of predicted and observed time to BF was made over the whole cohort. It included evaluation of matching BF events and their accuracy, as well as mismatches: predicted BF events that did not occur (false positives) and actual BFs that were not predicted (false negatives).

## RESULTS

Our mathematical mechanistic model adequately described PCa disease progression and response to ADT in HSPC. This minimum model consists of a tumor growth law with escalating growth rate, and emergence of resistance to ADT by two different biological mechanisms operating on two different time scales (Fig. 2). This model retrieved well the overall PSA dynamics in 83 HSPC patients under long-term follow-up ( $R^2 = 0.783$ , residual error of 0.576; Fig. 3A). Given the large differences in the PSA

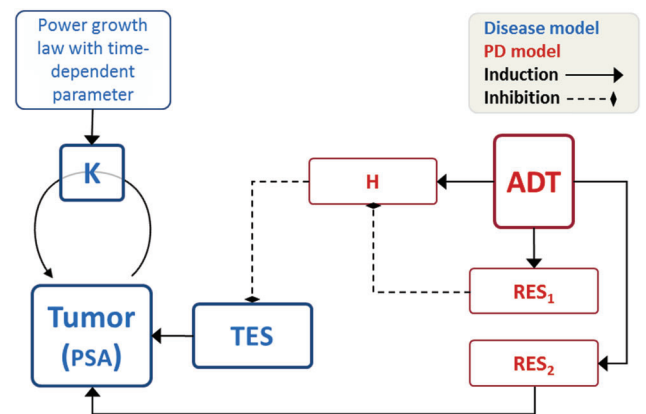


**Fig. 2.** Scheme of the mechanistic HSPC model. The ODE model for tumor progression in HSPC patients describes the PCa surrogate marker prostate-specific antigen (PSA), which grows by a power law with a variable coefficient ( $K$ ). PSA is controlled by the level of androgen, represented by testosterone (TES). Intervention by chemical or surgical castration, collectively termed androgen deprivation therapy (ADT), reduces the levels of TES indirectly, involving an intermediate factor ( $H$ ). Concomitantly, ADT instigates the rise of resistance ( $RES_1$ ) which interferes with its efficacy by reducing  $H$  levels. A second ADT-induced resistance effect ( $RES_2$ ) acts to increase PSA levels directly.

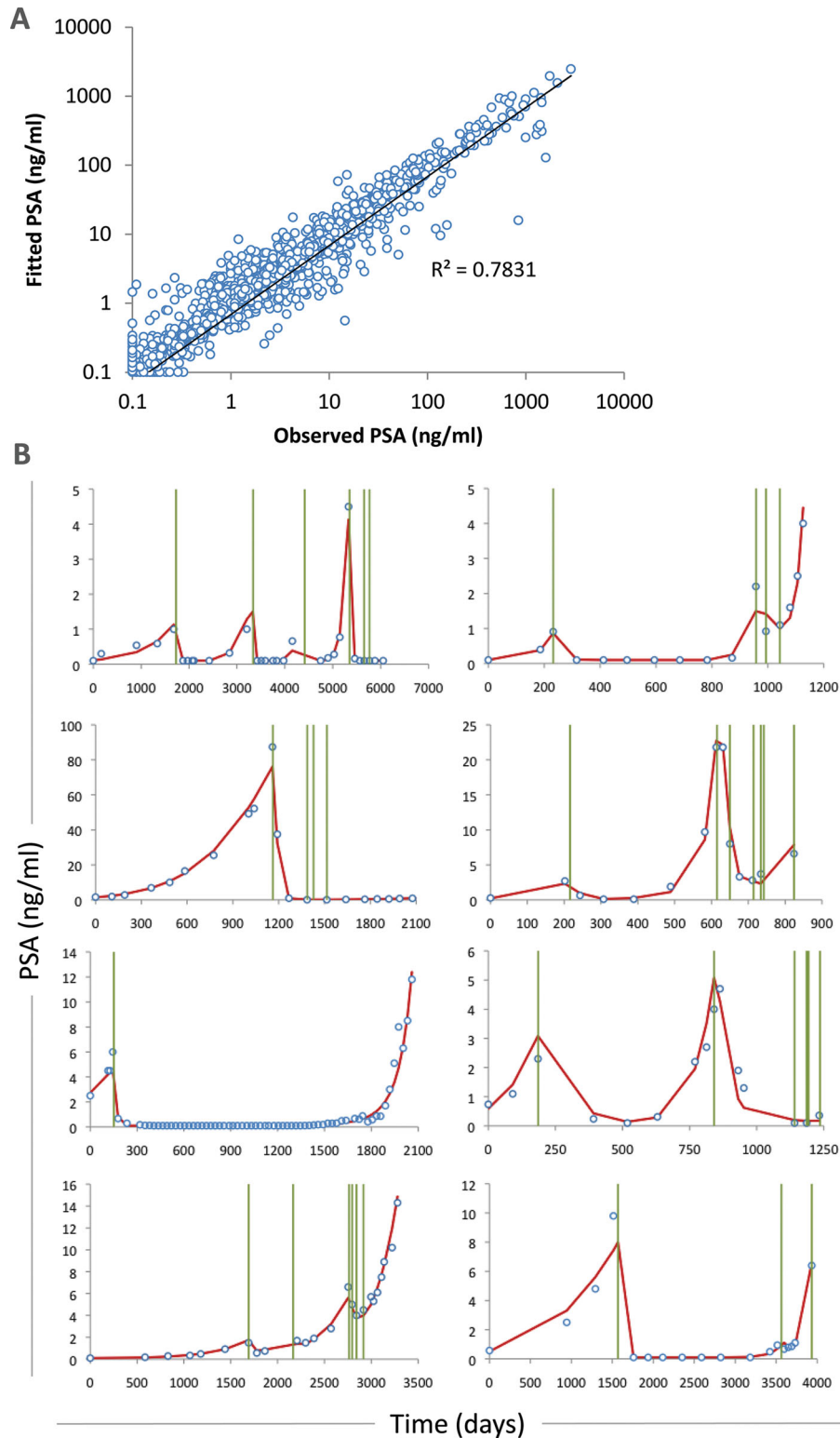


**Fig. 3.** Retrieval of individual PSA profiles by the mechanistic HSPC model. (A) Calibration of the mechanistic mixed-effects model using a dataset of longitudinal PSA profiles followed up during the HSPC stage in  $n=83$  PCa patients treated with ADT by diverse regimens. Goodness of fit plot, showing observed and model-fitted PSA values as log-transformed. (B) Model-fitted PSA profiles of 8 representative HSPC patients; observed PSA measurements (circles) are shown across model simulations (solid lines), with vertical lines indicating ADT administration times.

ranges among the patients, it was necessary to assume inter-individual variability in at least nine model parameters in order to capture the heterogeneous PSA dynamics (Supplementary Table SII). Individual model-data fits for eight representative patients demonstrate the quantitative and qualitative accuracy of model simulations (Fig. 3B).

Four model parameters were significantly associated with early clinical and pathological variables: PSA growth rate coefficient  $\lambda_1$  and the inverse growth limitation parameter  $\gamma$  were significantly correlated with the patient's GS (direct and inverse correlations, respectively). Likewise, resistance rate parameters were correlated to the PSA level at diagnosis (Supplementary Material, section A, Table SII). In a separate analysis, we also found that some of the mechanistic model parameters are potentially predictive factors for late clinical outcomes in HSPC patients, namely progression to CRPC and death: statistical time-to-event models (semi-parametric Cox PH and parametric regressions) surfaced a significant correlation between the PSA growth rate parameter  $\lambda_1$  and the ADT effect clearance rate parameter  $d_1$ , and time to CRPC onset and overall survival (Supplementary Material, section B).

We implemented the model in the personalization algorithm, and tested its power in predicting time to BF under ADT (a common defining event occurring toward progression to CRPC [16]) in individual patients. The personalization algorithm, employing the Bayesian approach, calculated personal model parameters using significant clinical metrics collected prior to treatment. It then simulated the personalized model to extract the patient's time to BF from the simulated PSA dynamics (Fig. 4A). Since some of the model parameters (i.e.,  $p$ ,  $\gamma$ , and  $\lambda_1$ ) were difficult to identify (as indicted in the RSE and CI of population values; Supplementary Table SII) due to the PSA variability, the algorithm required as input also a few PSA measurements collected over an initial period after treatment onset, in order to produce adequate curve fitting and better sampling of the conditional individual parameters values (Fig. 4A). We tested the ability of the personalization algorithm to retrieve the time to BF in the original HSPC dataset ( $n=83$ ), simulating the PSA dynamics of each patient under his retrospective ADT regimen (including ADT application times). Inputting the significant metrics (GS and PSA at diagnosis) and initial PSA data collected during the first 6 months after therapy initiation, the model successfully predicted 90% of the BFs (19/21 matches, two false negatives). In the matched events, the prediction accuracy of BFs was high ( $R^2=0.98$ ; Fig. 4B). The average difference between the observed

and predicted time to BF was only 67 days ( $SEM=18$ ; range of 0–271 days). Four false positive events were registered.

To examine whether the time to CRPC onset and OS in HSPC patients could also be predicted, statistical time-to-event models (both semi-parametric Cox PH and parametric regressions) were applied to evaluate the association between mechanistic model parameters and these two endpoints. Univariate analysis revealed four model parameters being significantly correlated ( $P < 0.05$ ) with time to CRPC by at least one regression model (Table II). Particularly, the clearance rate parameter of the ADT effect  $d_1$ , and the PSA growth rate parameter  $\lambda_1$ , were associated with a poor CRPC prognosis (Table II), as exemplified also in the Kaplan–Meier analysis (Fig. 4), and their prediction accuracy was verified by both leave-one-out cross validation and resampling (Table II). Importantly,  $\lambda_1$  was significantly correlated with OS, and a verified prognostic factor for poor outcome (Table II, Fig. 4). An independent analysis showed a number of clinically evaluated metrics in the HSPC patients that were also prognostic for time to CRPC and OS (see Supplementary Material, section B).

## DISCUSSION

An unmet clinical challenge in advanced PCa is the lack of a validated robust assay that is reproducible and reliable in predicting treatment response [5]. Today, multiple options are available for treatment of advanced PCa, including novel immunotherapies, hormone-based therapies, bone-targeted radioisotopes, and chemotherapies. As a result, matching treatment modality to the patient has become challenging. Unfortunately, recent therapeutic advances have occurred with no companion tools to evaluate their potential therapeutic benefit in individual patients. This deficiency has motivated the development of an alternative approach for predicting the response to ADT, based on a mathematical model-based personalization algorithm integrating standard clinical metrics.

The presented personalization algorithm focused on the clinically meaningful goal of predicting BF during therapy, after which patients are typically evaluated for CRPC progression and treated by therapeutics for this terminal stage. The algorithm accurately predicted BF in the retrospective HSPC cohort, by incorporating clinical information at diagnosis (GS and PSA), PSA collected during initial monitoring at the HSPC stage, and the ADT regimen actually applied to the patient. Notwithstanding the remarkable precision of our predictions, these results

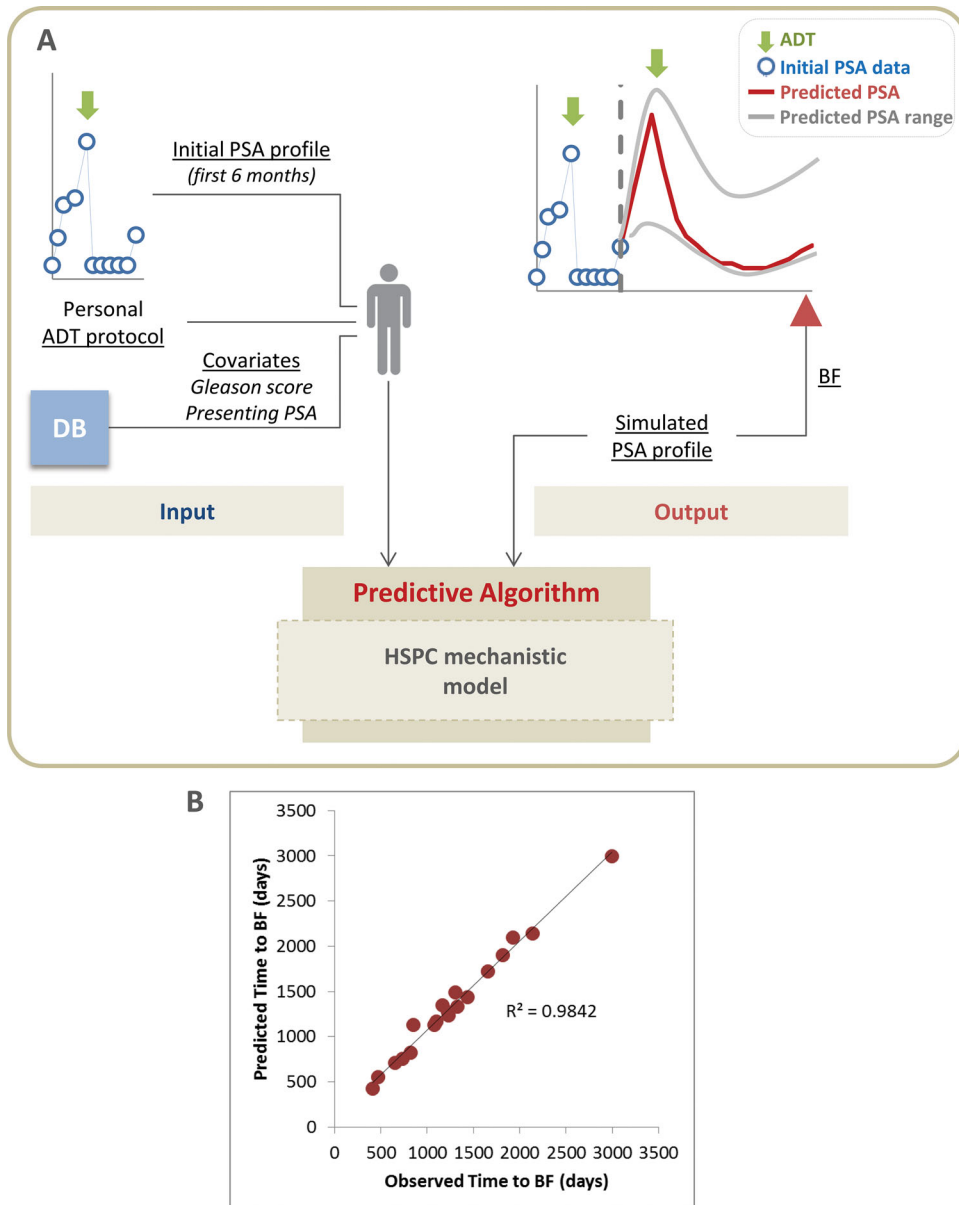


**Fig. 4.** Algorithm-predictions of biochemical failure in HSPC patients. (A) Scheme of the algorithm developed for simulating individual PSA profiles and deriving time to BF, based on the mechanistic HSPC model. Personal data of the initial PSA levels in a given HSPC patient (blue circles), and his individual covariate values (derived from the database; DB) and ADT regimen are input into the personalization algorithm. The algorithm then estimates the patient's individual parameter distributions using Bayesian inference, and simulates the mechanistic model for predicting PSA dynamics (Black line; range of predictions in grey lines) and BF occurrence (triangle) in that patient. (B) The algorithm's predictions of BF events in the retrospective  $n=83$  HSPC subset, using the approach described in panel (A). The matched algorithm-forecasted BF occurrences (19 events) are plotted vs. the observed BF events. An event is presented as time to BF in each patient;  $R^2$  is displayed.

should be taken with some precaution: because predictions of BF were validated retrospectively, the contribution of different types of information input cannot be evaluated at this stage. For example, the number of false positive events may have been underestimated due to the nature of this retrospective analysis: given that the simulated BF events were only

examined at the original PSA monitoring times (in order to compare them to the observed BF events), false positive events may have been overlooked in periods of no monitoring. Moreover, in HSPC, the ADT schedule is intertwined with the PSA sampling schedule and, consequently, with the observed PSA profile. In return, the observed PSA profile may

feedback on the ADT schedule. Therefore, a more accurate validation of the algorithm, done prospectively, will tackle this aspect by applying standard-of-care guidelines regarding ADT scheduling and PSA sampling.

Previously, we have demonstrated the potential of mathematical models to assist prediction of outcomes in the individual cancer patient and personalized planning of treatment, in the case of experimental vaccination immunotherapy for a small cohort of advanced PCa patients [8,9]. Using a simple mechanistic mathematical model which “learns” the patient during the initial treatment stage, and provides alternate regimens that can be applied immediately, we showed that a model-yielded treatment regimen would have improved the response in a number of patients [8]. The present work is another step forward in model-aided prediction of patient outcomes. By applying this strategy for an even larger hospital-based cohort of PCa patients under ADT, and by employing a more advanced modeling approach combining NLMEM and mechanistic models to realize this method, prediction of individual responses is attainable and accurate.

The mechanistic model of HSPC progression was developed by an integrative “bottom-up” and “top-down” approach, whereby the model was iteratively constructed based on biological mechanistic understanding of the system, and further adjusted by clinical PSA dynamics. Our suggested model is the minimal structure that could sufficiently well retrieve the data. Hence, the mechanistic aspects of the model represent the key processes underlying PCa dynamics and the resulting PSA behavior in advanced HSPC patients. In particular, the model highlights the complex PCa growth law, the rate of which increases over time. Indeed, it is acknowledged that the evolutionary dynamics of cancer cell populations subjected to therapy include ongoing selection of mutants that progressively increase the overall growth capacity of the population. The relatively long time periods over which such evolutionary dynamics operate in HSPC allow to discern these changes. Likewise, the emergence of failure on ADT appeared to require relatively complex modeling. Yet the fact that two mechanisms suffice to describe the development of castration resistance suggests that the multiple known biological resistance mechanisms [12,13] may be overlapping in function.

The mathematical mechanistic model may add insight into the dynamics of the system, which cannot be obtained by statistical analyses alone. Androgen resistance parameters were highly correlated with PSA level at diagnosis; this explains why the integration of PSA levels at diagnosis can aid in predicting

the timing of resistance onset, as exemplified in the accurate BF prediction by the algorithm. Similarly, the PSA growth rate parameter ( $\lambda_1$ ) was associated with GS, supporting the use of GS in determining the individual growth rate parameters and its contribution to disease severity. Indeed, prior reports present GS as an important prognostic measure for risk of ADT resistance [16] and risk of mortality [17]. Our mechanistic model-based algorithm thus extends the information value of these clinical markers (GS and initial PSA levels at diagnosis) beyond the past simple prognostic interpretations, integrating them for accurate prediction of the BF outcome.

The results of this work provide a proof-of-concept of the presented algorithm, yet a prospective clinical trial is mandatory for its clinical validation. In addition, various ADT protocols (different agents; different formulations; monotherapy or combination therapy combining anti-androgens and steroids) need to be implemented in the algorithm, and the ability to predict their differential efficacy should be studied. The algorithm must also consider inclusion of new drugs (i.e., abiraterone acetate and enzalutamide), which have shown promising response rates when applied together with ADT for HSPC patients with poor prognosis [5,18]. The use of our algorithm should also be considered not only for predicting early outcomes in individual HSPC patients, but also for assisting to forecast time to CRPC and survival. Given that prediction of such late outcomes in patients is critical for planning appropriate treatment, and realizing that biomarkers for these outcomes are still lacking [5,11,19], the prospect of using the algorithm to complement available prognostic markers is highly intriguing. In this context, the algorithm is adaptable to the dynamic biomarker realm in PCa: biomarkers that will be validated as having prognostic and predictive impact (e.g., circulating tumor cells) [5], and likely to be increasingly used within personalized PCa therapy in the years to come, can be easily included into the algorithm as covariates associated to dynamic model parameters, for the purpose of enhancing the prediction accuracy. Upon its prospective validation, the algorithm will, hopefully, be employed as a navigation decision-support tool for oncologists planning ADT or combined chemohormonal therapies for HSPC patients.

## CONCLUSIONS

We developed a personalization algorithm integrating clinical covariates with a mechanistic model for disease progression and ADT in HSPC patients. Predicting BF in a retrospective cohort of patients, based on routine clinical tests, could serve as a useful

tool for patients in this stage. In the future, this approach will, hopefully, assist in combining ADT with other novel therapies in patients destined to for quick progression to castrate resistance on single agent ADT alone.

### ACKNOWLEDGEMENTS

Conception and design: ME, YK, ZA. and MK. Data acquisition: MK, GHB, DN. and KMM. Literature search: ME, YK. and ZA. Mathematical modelling and simulations: ME and YK. Statistical analysis: IS. Drafting the manuscript: ME and ZA. Critical revision of the manuscript: ME, ZA. and MK. Final approval: ME, YK, IS, ZA. and MK. The authors thank S. Vuk-Pavlovic and I. F. Trocóniz for critically reviewing the manuscript, and Y. Kogan for helpful discussion. The study was supported by Joseph and Gail Gassner Development funds for prostate cancer research to MK.

### REFERENCES

- Horwitz EM, Bae K, Hanks GE, Porter A, Grignon DJ, Brereton HD, Venkatesan V, Lawton CA, Rosenthal SA, Sandler HM, Shipley WU. Ten-year follow-up of radiation therapy oncology group protocol 92-02: A phase III trial of the duration of elective androgen deprivation in locally advanced prostate cancer. *J Clin Oncol* 2008;26:2497–2504.
- Alva A, Hussain M. Intermittent androgen deprivation therapy in advanced prostate cancer. *Curr Treat Options Oncol* 2014; 15:127–136.
- Karantanos T, Corn PG, Thompson TC. Prostate cancer progression after androgen deprivation therapy: Mechanisms of castrate resistance and novel therapeutic approaches. *Oncogene* 2013;32:5501–5511.
- Kuhn E, Lavielle M. Coupling a stochastic approximation version of EM with an MCMC procedure. *ESAIM Probab Stat* 2004;8:115–131.
- Armstrong AJ, Eisenberger MA, Halabi S, Oudard S, Nanus DM, Petrylak DP, Sartor AO, Scher HI. Biomarkers in the management and treatment of men with metastatic castration-resistant prostate cancer. *Eur Urol* 2012;61:549–559.
- Agur Z, Arnon R, Schechter B. Reduction of cytotoxicity to normal tissues by new regimens of cell-cycle phase-specific drugs. *Math Biosci* 1988;92:1–15.
- Jain HV, Clinton SK, Bhinder A, Friedman A. Mathematical modeling of prostate cancer progression in response to androgen ablation therapy. *Proc Natl Acad Sci USA* 2011;108:19701–19706.
- Kogan Y, Halevi-Tobias K, Elishmereni M, Vuk-Pavlovic S, Agur Z. Reconsidering the paradigm of cancer immunotherapy by computationally aided real-time personalization. *Cancer Res* 2012;72:2218–2227.
- Kronik N, Kogan Y, Elishmereni M, Halevi-Tobias K, Vuk-Pavlovic S, Agur Z. Predicting outcomes of prostate cancer immunotherapy by personalized mathematical models. *PLoS ONE* 2010;5:e15482.
- Scher HI, Halabi S, Tannock I, Morris M, Sternberg CN, Carducci MA, Eisenberger MA, Higano C, Bubley GJ, Dreicer R, Petrylak D, Kantoff P, Basch E, Kelly WK, Figg WD, Small EJ, Beer TM, Wilding G, Martin A, Hussain M, Prostate Cancer Clinical Trials Working. Design and end points of clinical trials for patients with progressive prostate cancer and castrate levels of testosterone: Recommendations of the Prostate Cancer Clinical Trials Working Group. *J Clin Oncol* 2008;26:1148–1159.
- Kohli M, Qin R, Jimenez R, Dehm SM. Biomarker-based targeting of the androgen-androgen receptor axis in advanced prostate cancer. *Adv Urol* 2012;78:1459.
- Hussain M, Tangen CM, Berry DL, Higano CS, Crawford ED, Liu G, Wilding G, Prescott S, Kanaga Sundaram S, Small EJ, Dawson NA, Donnelly BJ, Venner PM, Vaishampayan UN, Schellhammer PF, Quinn DI, Raghavan D, Ely B, Moinpour CM, Vogelzang NJ, Thompson IM Jr. Intermittent versus continuous androgen deprivation in prostate cancer. *N Engl J Med* 2013;368:1314–1325.
- Pienta KJ, Bradley D. Mechanisms underlying the development of androgen-independent prostate cancer. *Clin Cancer Res* 2006;12:1665–1671.
- Kuhn E, Lavielle M. Maximum likelihood estimation in non-linear mixed effects models. *Comput Stat Data Anal* 2005; 49:1020–1038.
- Wallin JE, Friberg LE, Karlsson MO. Model-based neutrophil-guided dose adaptation in chemotherapy: Evaluation of predicted outcome with different types and amounts of information. *Basic Clin Pharmacol Toxicol* 2010;106:234–242.
- Fitzpatrick JM, Bellmunt J, Fizazi K, Heidenreich A, Sternberg CN, Tombal B, Alcaraz A, Bahl A, Bracarda S, Di Lorenzo G, Efstathiou E, Finn SP, Fossa S, Gill essen S, Kellokumpu-Lehtinen PL, Lecouvet FE, Oudard S, de Reijke TM, Robson CN, De Santis M, Seruga B, de Wit R. Optimal management of metastatic castration-resistant prostate cancer: Highlights from a European Expert Consensus Panel. *Eur J Cancer* 2014;50: 1617–1627.
- Rodrigues NA, Chen MH, Catalona WJ, Roehl KA, Richie JP, D'Amico AV. Predictors of mortality after androgen-deprivation therapy in patients with rapidly rising prostate-specific antigen levels after local therapy for prostate cancer. *Cancer* 2006;107:514–520.
- Shore ND, Abrahamsson PA, Anderson J, Crawford ED, Lange P. New considerations for ADT in advanced prostate cancer and the emerging role of GnRH antagonists. *Prostate Cancer Prostatic Dis* 2013;16:7–15.
- Kohli M, Riska SM, Mahoney DW, Chai HS, Hillman DW, Rider DN, Costello BA, Qin R, Lamba J, Sahasrabudhe DM, Cerhan JR. Germline predictors of androgen deprivation therapy response in advanced prostate cancer. *Mayo Clin Proc* 2012; 87:240–246.

### SUPPORTING INFORMATION

Additional supporting information may be found in the online version of this article at the publisher's web-site.